

## Effects of low surfactant Sb coverage on Zn and C incorporation in GaP

A. D. Howard and G. B. Stringfellow<sup>a)</sup>

*Department of Materials Science and Engineering, University of Utah, Salt Lake City, Utah 84112, USA*

(Received 20 March 2007; accepted 22 July 2007; published online 12 October 2007)

The use of surfactants during the vapor phase growth of III-V materials to control fundamental characteristics of epitaxial layers is becoming increasingly important. We have investigated the remarkable effects of Sb, from triethylantimony (TESb) pyrolysis, on the Zn doping during the organometallic vapor phase epitaxial growth (OMVPE) of GaP. Antimony is isoelectronic with the P host; therefore it is not a dopant in this material. It is also much larger than P so little incorporation occurs. We used secondary ion mass spectroscopy (SIMS) to investigate in detail the effects of TESb flow rate (Sb surface coverage) on the incorporation of the dopant Zn, as well as the background impurities C and H in GaP. The doping efficiency of Zn increased by as much as a factor of 2 when Sb was added during growth. Importantly, the observed effect was steady throughout the entire range of Sb levels from an Sb/III ratio of 0.01–0.05. Previous studies indicate that this would yield Sb surface coverages of 0.3 (for Sb/III=0.01) to 0.65 (for Sb/III=0.05). Thus, the Sb surface coverage is not saturated. Other results indicate that Sb coverage may be higher at the step edge, which suggests that the surfactant effect on Zn doping occurs at the step edge. Additionally, Sb caused an increase in the hydrogen concentration and a reduction in the carbon contamination. We propose a simple mechanism for the surfactant effect on Zn doping due to an increase of Sb coverage near the step edge. © 2007 American Institute of Physics. [DOI: [10.1063/1.2778635](https://doi.org/10.1063/1.2778635)]

### I. INTRODUCTION

It has recently become apparent that control of the surface structure during vapor phase epitaxial growth is an important tool in controlling the growth process itself, as well as the properties of the resultant epitaxial layers.<sup>1</sup> A prime example is the use of surfactants, such as Sb, to control atomic-scale ordering in GaInP grown by organometallic vapor phase epitaxy (OMVPE).<sup>2,3</sup> Thus, the use of surfactants isoelectronic with the host material, which do not act as either a donor or acceptor, provides a convenient method for band gap control in commercial devices such as solar cells<sup>4–6</sup> and light emitting diodes.<sup>7</sup> Other studies have led to the discovery that such surfactants can also be used to control the incorporation of dopants as well as unintentional impurities.<sup>8–12</sup>

The mechanisms controlling the effects of surfactants on dopant incorporation are only beginning to be understood. In fact, dopant incorporation processes in general are not well understood. Simple thermodynamic<sup>13</sup> and kinetic<sup>14</sup> arguments provide an outline of the basic processes; however, the details are unclear. Dopant incorporation may occur by simple exchange reactions at flat surfaces<sup>15</sup> or at steps on the surface.<sup>14</sup> The latter involves the additional complication of knowing the step structure, including both the occurrence of step bunching and the presence and concentration of particularly active step sites such as kinks. All of these complexities call for a combination of theory and detailed experiments to understand and control the basic processes at work in surfactant mediated dopant incorporation.

This article describes work designed to explore in detail

the use of the surfactant Sb to enhance Zn incorporation in GaP grown by OMVPE. Recent work<sup>5,6</sup> has indicated that the surfactant effect of Sb to reduce ordering in GaInP occurs at such low Sb surface coverage that formerly well-accepted mechanisms involving Sb effects on surface composition and reconstruction<sup>1</sup> may not be dominant. This work has been interpreted to suggest the importance of Sb at step edges.<sup>6</sup> Batyrev *et al.*<sup>16</sup> showed that it is energetically more favorable for Sb to occupy step sites than surface sites on GaP. This would result in the saturation of the Sb coverage at the step edge at lower TESb partial pressures than necessary for saturation of Sb coverage on the singular regions between steps. Limited experimental data on the effects of Sb on ordering in GaInP (Ref. 6) grown by OMVPE is interpreted to show a reduction in ordering when the Sb fractional surface coverage is as low as 0.003, although no experimental details were provided. The present work explores Sb effects on dopant incorporation during OMVPE growth at low Sb concentrations in the vapor giving surface coverage of less than one.

### II. EXPERIMENT

GaP layers doped with Zn were epitaxially grown with the presence of surfactant Sb by OMVPE in a horizontal, infrared-heated, atmospheric pressure reactor on singular (001) semi-insulating GaP substrates. Trimethylgallium (TMGa), tertiarybutylphosphine (TBP), dimethylzinc (DMZn), and triethylantimony (TESb) were used as the organometallic precursors. The carrier gas was Pd-diffused hydrogen. Throughout the experiments a constant growth rate of 1  $\mu\text{m/h}$  was maintained. The samples were grown at 650 °C with a V/III ratio of 60. The TESb/TBP ratios used were: 0,  $9.23 \times 10^{-5}$ ,  $1.88 \times 10^{-4}$ ,  $2.85 \times 10^{-4}$ ,  $3.8 \times 10^{-4}$ , and  $4.5 \times 10^{-4}$ .

<sup>a)</sup>Author to whom correspondence should be sent. Electronic mail: [stringfellow@coe.utah.edu](mailto:stringfellow@coe.utah.edu)

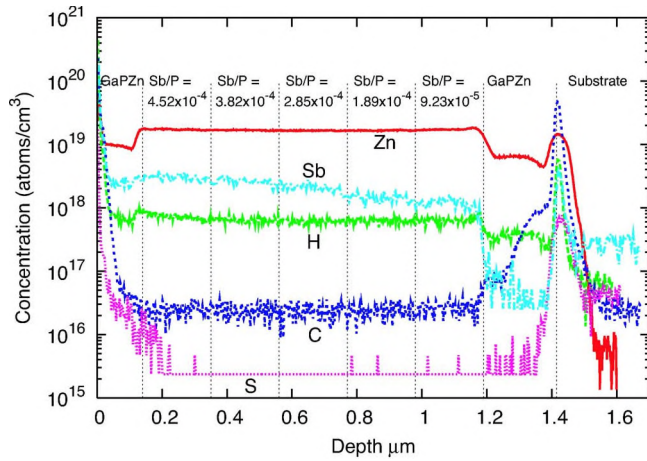


FIG. 1. (Color online) SIMS profile for a seven-layer GaP structure grown at 650 °C. Each layer was grown with a different Sb/P ratio as indicated.

Atomic force microscopy (AFM) was used to determine the effect of Sb on step structure. A Digital Instrument Dimension 3000 system was used in tapping mode with etched Si tips having a 5 nm radius.

At each interface in the multilayered sample, growth was interrupted for 60 s to allow flows to stabilize. Evans Analytical Group measured SIMS depth profiles, using a Cameca IMS4f magnetic sector SIMS instrument. A Cs<sup>+</sup> ion beam was used to erode the sample for depth profiling. Data were collected using both positive and negative detection conditions. The results were calibrated using GaP standards implanted with known doses of the elements of interest. The depth scale was calibrated based on the depth of the SIMS craters.

### III. RESULTS AND DISCUSSION

The addition of Sb (TESb) during the growth of GaP and GaInP materials was previously shown to dramatically alter the doping characteristics.<sup>11,12</sup> The recent results of Olsen *et al.*<sup>6</sup> on disordering at very low surface coverage suggests the need for a closer inspection of how much surfactant is required to affect Zn doping. In an effort to more clearly define the mechanism, we focused on low temperature (650 °C) growth with surfactant Sb surface coverage of less than one.

To investigate the effects of lower Sb partial pressures on Zn doping, a seven-layered structure was grown at 650 °C. The SIMS depth profile is shown in Fig. 1. The TESb flow rate was varied over a wide range and the top and bottom layers were grown without any TESb added. The surfactant effect observed here is similar to previous results.<sup>11,12</sup> The SIMS profile clearly shows that the Zn doping is enhanced by the presence of Sb. However these data reveal the surprising fact that the amount of Zn incorporated is nearly independent of the TESb flow rate during growth, i.e., the surfactant enhancement of Zn doping saturates at the lowest TESb flow rate. Additionally, the surfactant effect of Sb on C and H is also shown to be constant throughout the layers. Thus, despite the change in Sb present during growth, Zn and H incorporation increase while the C decreases and the magnitude of the effect is independent of the TESb flow.

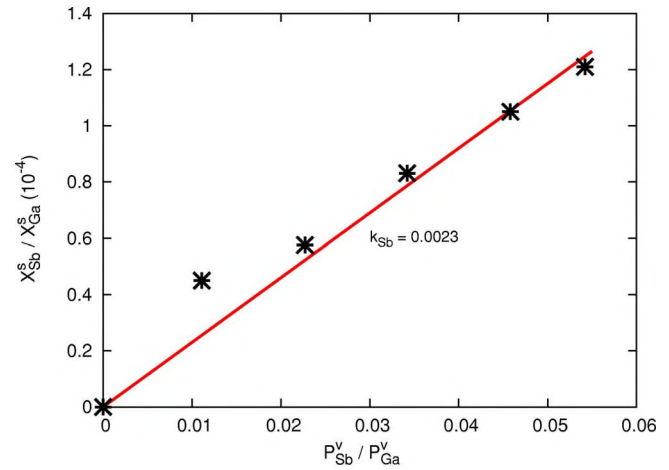


FIG. 2. (Color online) The Sb concentration in the solid normalized by the Ga in the solid versus the concentration ratio of the input partial pressure of TESb to TMGa for GaP grown at 650 °C.

In contrast, as seen in Fig. 2, the concentration of Sb in the solid is a linear function of the TESb input partial pressure over the entire range studied. The amount of antimony incorporated into the solid is much less than 0.01%. The slope of the line allows determination of the antimony distribution coefficient,  $[x_{\text{Sb}}/x_{\text{Ga}}]/[p_{\text{Sb}}/p_{\text{Ga}}]$ . Here,  $x$  represents the mole fraction in the solid and  $p$  the input partial pressure of the relevant precursor. Note that the curve is constrained to go through the origin. The experimental value determined from a least-squares fit of the data in Fig. 2 is 0.0023. For a nonvolatile dopant, which cannot escape from the surface, the distribution coefficient defined in this way should be unity.<sup>13</sup> This is consistent with the behavior previously reported for As/Sb alloys.<sup>17</sup> Clearly Sb is leaving the surface before incorporation into the solid even though it has a low elemental vapor pressure. It is likely that Sb bonds with the available atomic H on the surface and volatilizes as SbH<sub>3</sub>. Thus, the effect of Sb on Zn, H, and C concentrations is even more intriguing. The contrast is clearly shown in Fig. 3, where the concentrations of both Zn and Sb in the solid are plotted versus the input TESb partial pressure. Sb doping

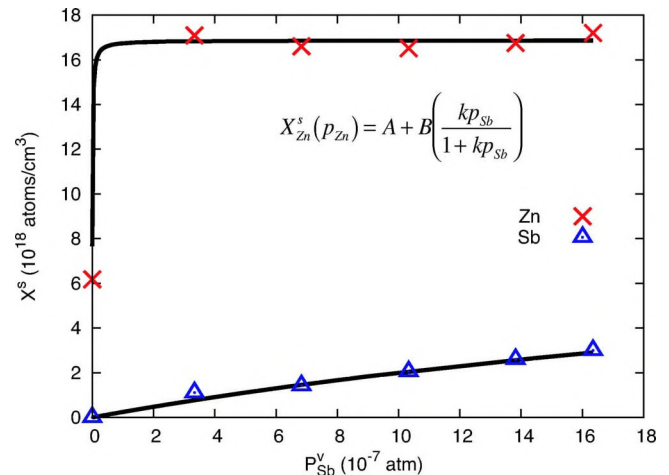


FIG. 3. (Color online) The concentration of dopant Zn in GaP grown at 650 °C with a proposed fit line that corresponds to surfactant coverage at the steps.

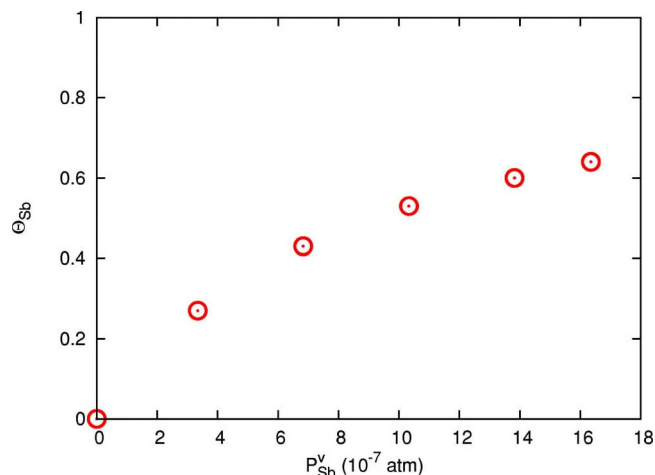


FIG. 4. (Color online) Surface coverage of surfactant Sb versus the partial pressure of Sb in the vapor, from the GaInP (620 °C) data of Shurtleff *et al.* (Ref. 18).

presumably occurs by Sb/P exchange reactions over the entire surface, thus giving the classic linear dependence seen in Fig. 3. Incorporation of dopants is normally considered to occur at the step edge.

The saturation of the Sb effect on Zn doping, clearly seen in Fig. 3, can be interpreted in terms of the saturation of Sb surface coverage at the positions on the surface where Zn is incorporated, most likely at step edges. Thus, the saturation of the surfactant effect on Zn incorporation appears to indicate that the surface regions near the step edge have a much higher Sb coverage than the singular areas between steps.

The surface coverage on the singular surface can be estimated from kinetic data of Shurtleff *et al.*<sup>18</sup> for GaInP at 620 °C based on surface photoabsorption measurements, which sample the singular (100) regions between steps. The fractional surface coverage calculated from their data is shown in Fig. 4. The maximum value is 0.65. One expects a

lower value for the GaPZn:Sb surface in this article, since the temperature is higher. Thus, we conclude that the (100) regions of the surface are not saturated with a monolayer of Sb even at the highest TESb flow rates.

This analysis leads to the conclusion that the Sb surface coverage at the step edge is higher than on the (100) regions between the steps. This is supported by the work of Olson *et al.* and Batyrev *et al.*<sup>6,16</sup> The former showed that disorder (of the CuPt structure) by Sb occurs at very low Sb surface coverage. The latter showed theoretically that Sb is attracted to step edges.

A second hypothesis must also be examined, namely that the increased Zn incorporation due to the presence of Sb could be attributed to an indirect effect related to a change in step structure. To evaluate this possibility, the surface structure was examined by AFM. Figure 5 shows AFM scans and images from singular samples with (Sb/P=4.5 × 10<sup>-4</sup>), Fig. 5(b), and without, Fig. 5(a), Sb present during growth. The (110) cross sections are shown below the images to illustrate the effect of Sb on the step structure. The contrast between samples with and without Sb is striking. The addition of Sb apparently causes the steps to bunch, resulting in an increase in the overall roughness for these singular substrates. This increase in step density will decrease the step velocity during growth. Previous work has shown that a decrease in step velocity will reduce Zn incorporation due to a decrease in Zn trapping at the step edge.<sup>19</sup> We clearly see an increase in Zn incorporation (Fig. 1); therefore it is unlikely that the surfactant effect observed is due to the step structure induced by Sb. It should also be noted that the addition of Sb has no effect on the GaP growth rate.

Taken together, the above experimental data indicate that it is the Sb surface coverage of the regions near the step edges that controls Zn incorporation. A simple model has been developed to explain the dependence of Zn incorpora-

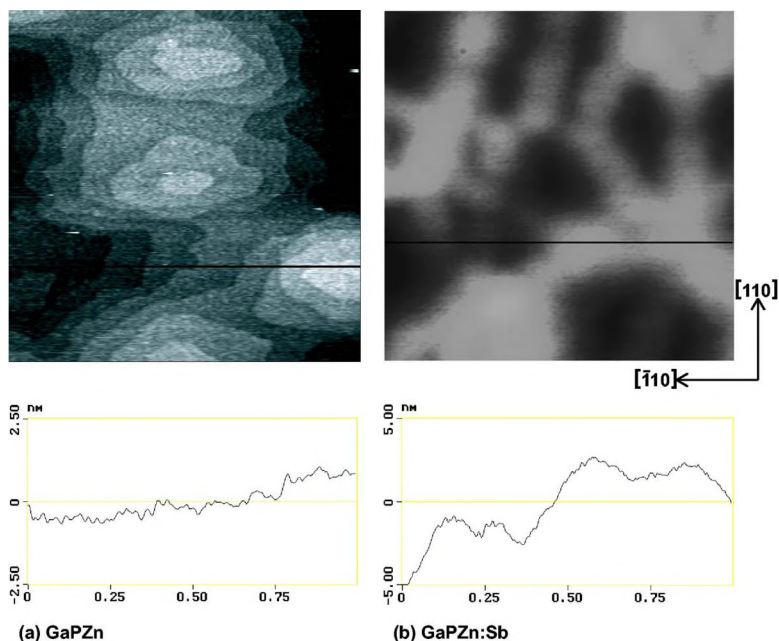


FIG. 5. (Color online) AFM images of (a) GaPZn and (b) GaPZn:Sb (Sb/P=4.5 × 10<sup>-4</sup>) grown on singular substrates at 650 °C. The (110) cross sections were obtained across the black lines in the AFM images.



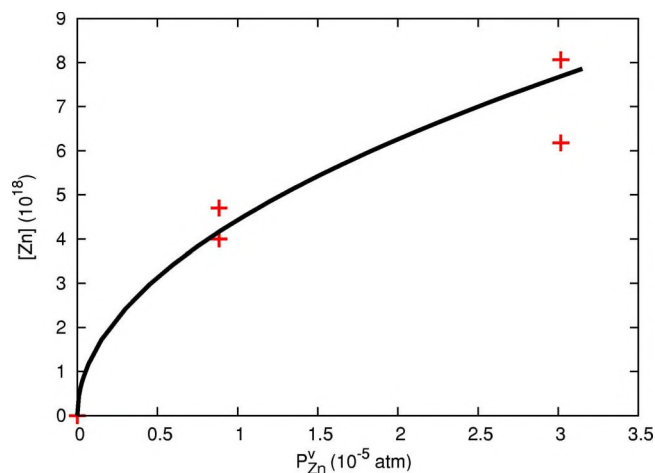


FIG. 6. (Color online) The concentration of Zn in the solid plotted versus the partial pressure of DMZn for GaP grown at 650 °C. The data yield a value for  $A$  in Eq. (2) of 7.67.

tion on the input TESb partial pressure. Antimony adsorption and desorption rates are balanced at the steady state, yielding the Langmuir isotherm<sup>20</sup> for Sb

$$\Theta_{\text{Sb}} = \frac{k p_{\text{Sb}}}{1 + k p_{\text{Sb}}}. \quad (1)$$

The constant  $k$  is simply the ratio of the rate constants for adsorption and desorption. For simplicity, the effect of Sb on Zn incorporation into the solid will be taken as a linear function of antimony coverage at the step edge

$$k_{\text{Zn}}^{\text{incorporation}} = A + B \Theta_{\text{Sb}}^{\text{Step}}. \quad (2)$$

This implicitly assumes that the incorporation rate constant is much smaller than that for desorption, which is dictated by the small antimony distribution coefficient.

The value of  $A$  is determined by the Zn incorporation behavior with no Sb present during OMVPE growth using the conditions (temperature, V/III ratio, and growth rate) used in this study. Previous studies have demonstrated a square-root dependence of Zn incorporation on the input partial pressure of the Zn precursor.<sup>21</sup> The value of Zn mole fraction in the solid is plotted versus the partial pressure of the Zn precursor, DMZn, in Fig. 6. The best fit to our experimental data assuming this square-root dependence and that the curve intersects the origin is shown as the solid line. This yields a value of  $A$  in Eq. (2) of 7.67 for the constant Zn partial pressure used in these experiments. The saturation value of Zn concentration in Fig. 3 determines the value of the constant  $B$  in Eq. (2) to be 9.2. This leaves only the constant  $k$  to be determined by fitting the experimental data. The solid line shown in Fig. 3 was calculated, using the equation shown in the inset [the result of combining Eqs. (1) and (2)], using a value of  $k = 7 \times 10^8$ . This is the lower limit. It could be larger without affecting the fit to the experimental data. Thus, the absence of data at low values of TESb partial pressure makes this value of  $k$  quite uncertain.

The effect of surfactant Sb on carbon incorporation is opposite to that of Zn, as seen in Fig. 7. However, saturation of the surfactant effect suggests that the mechanism also in-

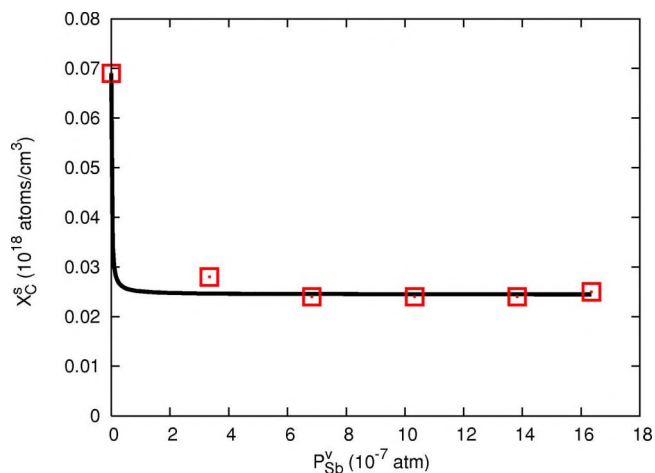


FIG. 7. (Color online) The effect of surfactant Sb on the concentration of carbon incorporated into the solid at 650 °C. The solid line was fit to the data using the value of  $k$  determined from the Zn data.

volves Sb adsorption near the step edge. Two possible interpretations of the data are: (1) Sb on the surface acts to decrease the incorporation rate for C, thus decreasing C incorporation into the solid, or (2) The reduction of C incorporation is due to an increase in the C (most likely CH<sub>4</sub>) desorption from the step region, thus decreasing the surface coverage of C near the step edge as discussed in a previous work.<sup>12</sup> Assuming that the case<sup>1</sup> described above, the C incorporation would follow the same form observed for Zn, with the exception that the constant  $B$  in Eq. (2) is different, in fact negative, for carbon. The solid line in Fig. 7 was calculated in this way, using the value of  $k$  determined for Zn as described above. It provides a good fit to the experimental data, suggesting that the surfactant mechanisms both involve Sb coverage at the step edge.

#### IV. SUMMARY

These results demonstrate that the surfactant Sb, isoelectronic with host P, increases the Zn and H incorporation while decreasing the background C concentration in epitaxial layers of GaP. Furthermore, we demonstrate that the surfactant effect is independent of TESb flow rate over the range investigated, which give surface coverage of less than one. We suggest that the effect is due to the saturation of Sb at the step edge and not on the singular (001) regions of the surface. We have developed a simple step model to describe the phenomena.

#### ACKNOWLEDGMENT

The authors wish to thank the Department of Energy, Division of Basic Energy Sciences, for support of this work.

<sup>1</sup>G. B. Stringfellow, J. K. Shurtleff, R. T. Lee, C. M. Fetzer, and S. W. Jun, *J. Cryst. Growth* **221**, 1 (2000).

<sup>2</sup>J. K. Shurtleff, R. T. Lee, C. M. Fetzer, and G. B. Stringfellow, *Appl. Phys. Lett.* **75**, 1914 (1999).

<sup>3</sup>G. B. Stringfellow, R. T. Lee, C. M. Fetzer, J. K. Shurtleff, Y. Hsu, S. W. Jun, S. Lee, and T. Y. Seong, *J. Electron. Mater.* **29**, 134 (2000b).

<sup>4</sup>C. M. Fetzer, J. H. Ermer, R. R. King, and P. C. Cotler, U. S. Patent No. 7,122,734 B2 (17 October 2006).

<sup>5</sup>C. M. Fetzer, J. H. Ermer, R. R. King, and P. C. Cotler, U. S. Patent No.

- 7,126,052 B2 (24 October 2006).
- <sup>6</sup>J. M. Olson, W. E. McMahon, and S. Kurtz, in *4th World Conference on Photovoltaic Energy Conversion* (IEEE, Waikoloa, HI, 2006), p. 787.
- <sup>7</sup>S. Tanaka, J.-S. Lee, P. Ramvall, and H. Okagawa, *Jpn. J. Appl. Phys., Part 2* **42**, L885 (2003).
- <sup>8</sup>J. K. Shurtleff, S. W. Jun, and G. B. Stringfellow, *Appl. Phys. Lett.* **78**, 3038 (2001).
- <sup>9</sup>F. Dimroth, A. Howard, J. K. Shurtleff, and G. B. Stringfellow, *J. Appl. Phys.* **91**, 3687 (2002).
- <sup>10</sup>Z. H. Feng, H. Yang, S. M. Zhang, L. H. Duan, H. Wang, and Y. T. Wang, *J. Cryst. Growth* **235**, 207 (2002).
- <sup>11</sup>D. C. Chapman, A. D. Howard, and G. B. Stringfellow, *J. Cryst. Growth* **287**, 647 (2006).
- <sup>12</sup>A. D. Howard, D. C. Chapman, and G. B. Stringfellow, *J. Appl. Phys.* **100**, 044904 (2006).
- <sup>13</sup>G. B. Stringfellow, *Organometallic Vapor-Phase Epitaxy: Theory and Practice*, 2nd ed. (Academic, San Diego, 1999a), pp. 91–95.
- <sup>14</sup>G. B. Stringfellow, *Organometallic Vapor-Phase Epitaxy: Theory and Practice*, 2nd ed. (Academic, San Diego, 1999b), pp. 142–144.
- <sup>15</sup>J. A. Venables, in *Thin Films: Heteroepitaxial Systems*, edited by W. K. Liu and M. B. Santos (World Scientific, New Jersey, 1999), p. 1.
- <sup>16</sup>I. G. Batyrev, W. E. McMahon, S. B. Zhang, J. M. Olson, and S.-H. Wei, *Phys. Rev. Lett.* **94**, 096101 (2005).
- <sup>17</sup>G. B. Stringfellow, *Organometallic Vapor-Phase Epitaxy: Theory and Practice*, 2nd ed. (Academic, San Diego, 1999b), pp. 445–452.
- <sup>18</sup>J. K. Shurtleff, R. T. Lee, and G. B. Stringfellow, in *Proceedings of the IEEE Twenty-Seventh International Symposium on Compound Semiconductors* (IEEE, Monterey, CA, 2000), pp. 197–203.
- <sup>19</sup>P. R. Hageman, J. te Nijenhuis, M. J. Anders, and L. J. Giling, *J. Cryst. Growth* **170**, 270 (1997).
- <sup>20</sup>I. Langmuir, *J. Am. Chem. Soc.* **40**, 1361 (1918).
- <sup>21</sup>R. W. Glew, *J. Cryst. Growth* **68**, 44 (1984).